

A local power law versus a well-identified viscosity curve over a large shear rate range in thermorheology of polymers

LIN Qiao^{1,a,*}, ALLANIC Nadine^{1,b}, MOUSSEAU Pierre^{1,c}, BERAUX Yves^{1,d},
GIRAULT Manuel^{2,e} and DETERRE Rémi^{1,f}

¹GEPEA Nantes Université, Oniris, CNRS, GEPEA, UMR 6144, F-44000 Nantes, France

²Institut P' CNRS-ENSMA-Université de Poitiers, UPR 3346, F86961 Futuroscope Chasseneuil Cedex, France

^aqiao.lin@univ-nantes.fr, ^bNadine.Allanic@univ-nantes.fr, ^cpierre.mousseau@univ-nantes.fr,
^dyves.beraux@univ-nantes.fr, ^emanuel.girault@ensma.fr, ^fremi.deterre@univ-nantes.fr

Keywords: Pseudo-Plastic; Annular Flow; Cross Law; Viscous Dissipation; Velocity Field

Abstract. There are always debates on the use of power law to model flows having a local zero shear rate. This paper uses an original method to define a functional shear rate range with respect to the flow condition and identify an equivalent power law from a Cross-law fluid. The numerical and experimental results are compared to show the ability of the power law to model a flow having a low-shear region.

Introduction

Different viscosity models exist to represent the rheology behavior of polymers. The most simple behavior law for non-Newtonian materials is the power law [1,2]. The shortcoming of the power-law model to describe the viscosity at the zero shear rate was pointed out by several studies [3,4]. Some authors claim that the power law can be used with particular attention to the shear stress range [5], while some just use more complex models such as the Cross model [6] and the Carreau model [7] which better describe the low-shear regime.

The power law cannot be totally abandoned. Although the simplifications that the power law (compared to other complex viscosity models) can provide in numerical studies may seem small, it can still bring clarity for sensitivity analyzes [8] or facilitate the development of analytical formulations. It is important to know whether the power law can be used when a low-shear region exists in the flow.

In this paper, a power law, fitted to a Cross law for a specific shear rate range by an innovative thermo-rheological method [8], is used to model an annular polymer flow. The Cross law is also used to model the same flow for comparison. An experimental annular device [9] is used to measure the flow temperature variation due to viscous dissipation. The temperature measurements are compared to the predictions of the viscosity models. The numerical simulation results for the shear rate, viscosity, shear stress and velocity in the flow are compared as well.

Flow Geometry

We propose to perform analyzes on an annular polymer flow, which can be studied by using a Thermo-Rheo Annular Cell (TRAC) [9]. The structure of the TRAC is presented in Fig. 1, with thermocouples T_{1-4} installed on its central axis for flow temperature measurements. The polymer flow enters the duct from the left of the figure and is guided to the annular part ($z \geq 0$) by a 45° cone. The outlet is on the right side (Fig. 1). The central axis is not only for thermocouple instrumentation, but also for generating additional viscous dissipation in the passing flow, to extract information from the rheological behavior of the flow. The details on the flow model of the TRAC can be found in [9].



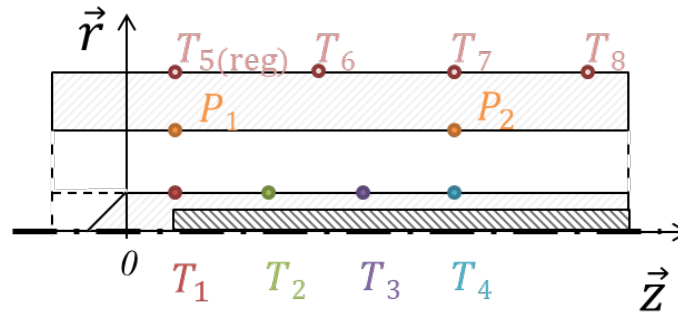


Fig. 1. Illustration of the TRAC.

Viscosity Models

The Cross law [6] (Eq. 1) is employed to represent the rheological behavior of the polymer :

$$\eta = \eta_0 / \left[1 + \left(\frac{\eta_0}{\tau^*} \dot{\gamma} \right)^{1-n} \right] \quad (1)$$

with η the viscosity, $\dot{\gamma}$ the generalized shear rate, η_0 the zero shear rate viscosity, n the power index at high shear rate regime ($0 < n < 1$ for shear thinning materials such as the polymers) and τ^* the critical stress level at the transition to shear thinning. According to the material database of the « Autodesk® Moldflow® » software, the Cross-law parameters for Polypropylene PPC 9642 at 195 °C are: $\eta_0 = 3192.75$ Pa.s, $\tau^* = 19996.2$ Pa and $n = 0.3387$.

The power law [1,2], shown in Eq. 2, is used to compare to the Cross law.

$$\eta = K \dot{\gamma}^{n_p - 1} \quad (2)$$

with K the consistency coefficient and n_p the power-law index ($0 < n_p < 1$ for shear thinning materials). The power law is a straight line in logarithmic scale having the slope: $(d \ln \eta / d \ln \dot{\gamma} = n_p - 1)$. It should be noted that the Cross law also has a similar slope for $\dot{\gamma} \rightarrow \infty$: $\left(\lim_{\dot{\gamma} \rightarrow \infty} d \ln \eta / d \ln \dot{\gamma} = n - 1 \right)$. The power-law parameters (K and $n_p \neq n$) are carefully chosen to compare with the Cross law of PPC 9642. This is detailed in the next section.

Procedure of the Study

A power-law curve can be drawn from two different viscosity points. In this paper, we use an innovative method to obtain viscosity points from temperature measurements. When the polymer melt flows through the TRAC, the temperature variation due to viscous dissipation is recorded at the central axis of the annular geometry. This temperature variation, for a given flowrate, is sensitive to one point on the material's viscosity curve. The point is called « critical point » in [8]. To identify critical points, the inverse method process can be designed with different approaches. But the process always takes temperature signals as the input variables and a critical point for each flowrate as the output result. Higher flowrates lead to critical points at higher shear rate regime. We need two different flowrates to obtain two critical viscosity points.

In practice, the TRAC is installed as a nozzle at the outlet of an injection unit. During injection, the polymer flows through the TRAC. Experiments are carried out with Polypropylene PPC 9642 at two different injection flowrates: $42.4 \text{ cm}^3 \cdot \text{s}^{-1}$ and $56.5 \text{ cm}^3 \cdot \text{s}^{-1}$. The corresponding simulations are brought off using the finite element model of the TRAC and the Cross-law viscosity model of the same polymer.

The main discussion of this study is whether the power law can perform as well as a more complex viscosity model rather than the identification of material parameters. To find an equivalent power-law curve of the Cross-law one, the identification of the power-law parameters is performed from the results of the simulations with the Cross law, that is to say by using the simulated temperature variation as a reference (Fig. 2). Two critical viscosities ($580.3 \text{ Pa}\cdot\text{s}$ - 61.7 s^{-1} and $500.6 \text{ Pa}\cdot\text{s}$ - 80.5 s^{-1}) are obtained by applying the inverse method on the Cross-law simulation results, respectively at a flowrate of $42.4 \text{ cm}^3\cdot\text{s}^{-1}$ and $56.5 \text{ cm}^3\cdot\text{s}^{-1}$. A power-law curve ($K = 5721.2 \text{ Pa}\cdot\text{s}^n$, $n = 0.4448$) is drawn from these two points in Fig. 3.

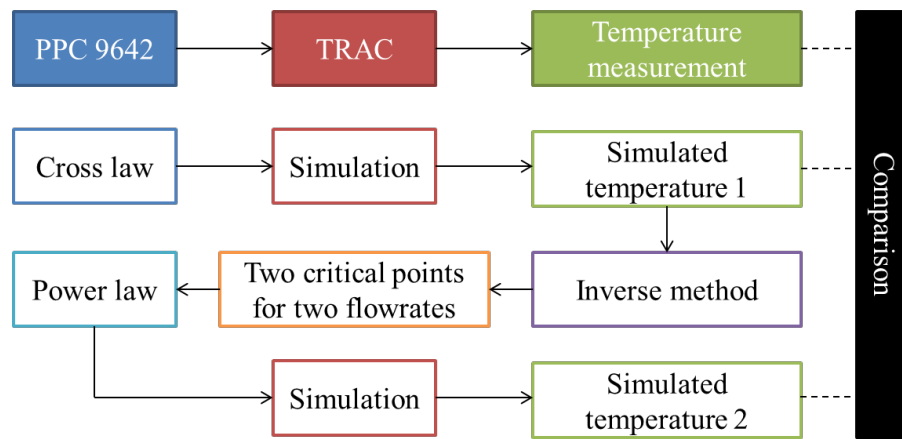


Fig. 2. Procedure of the study.

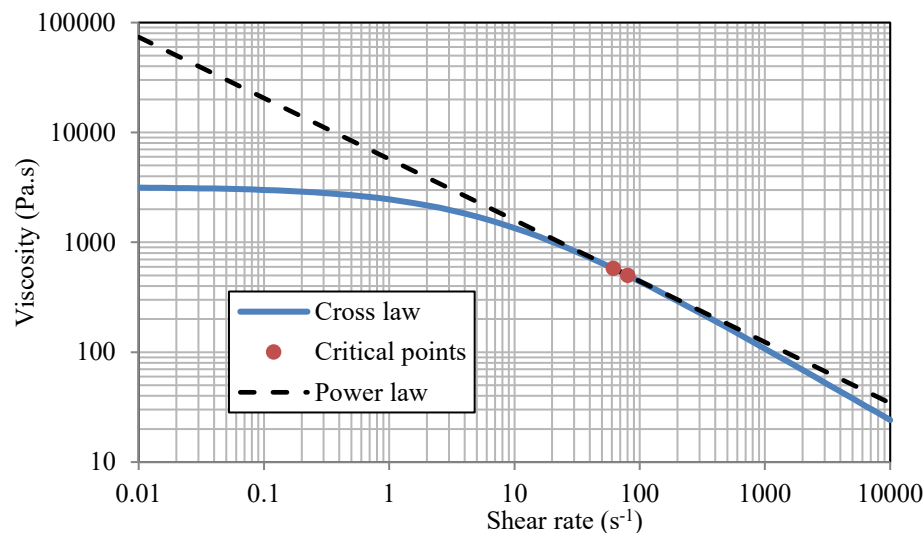


Fig. 3. Viscosity curves of the Cross law and the power law along with the critical points.

Fig. 3 shows that the critical points are on the Cross-law curve, because they are obtained from the Cross-law simulation results. The power-law curve, passing through the critical points, is close to the Cross-law curve only in a specific zone, near the transition region between the low-shear Newtonian zone and the high-shear pseudo-plastic zone. The difference between the two viscosity models can be seen at the high shear rate regime and especially at the low shear rate regime.

Other simulations at the same flowrates are carried out by using the power-law curve in Fig. 3 to replace the Cross-law viscosity model. In the next section, we will find out whether the power-law curve is good enough to describe the flow behavior and whether the critical viscosity points can represent a functional zone of a viscosity curve, by comparing the measurements of the TRAC,

the Cross-law simulations' results and the power-law simulations' results (Fig. 2). The simulation software used is « ANSYS® POLYFLOW® ». Shear rate, velocity and temperature profiles can be exported directly from the simulation tool. The viscosity and shear stress profiles are calculated from the shear rate profiles using analytical expressions (Eq. 1 and Eq. 2).

Results and Discussion

ΔT is the temperature variation relative to that of the initial state. The temperature variations ΔT due to viscous dissipation during injection (at $42.4 \text{ cm}^3 \cdot \text{s}^{-1}$ and $56.5 \text{ cm}^3 \cdot \text{s}^{-1}$) are measured directly by the TRAC and shown in Fig. 4. For an easy reading of the figure, only the temperatures measured by thermocouples T_2 and T_4 (Fig. 1) are presented. These flow configurations are also simulated with the Cross law and the power law. The results of the simulations are presented in Fig. 4 as well.

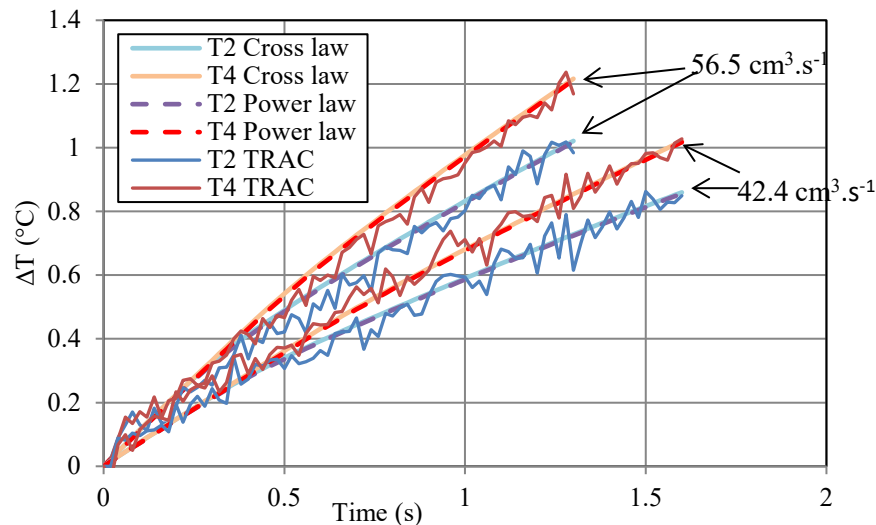


Fig. 4. Temperature variations (due to viscous dissipation during injection) measured by thermocouples T_2 and T_4 of the TRAC and simulated with the Cross law and the power law for different flowrates ($42.4 \text{ cm}^3 \cdot \text{s}^{-1}$ and $56.5 \text{ cm}^3 \cdot \text{s}^{-1}$).

The increase in temperature due to viscous dissipation can be observed in Fig. 4. The higher the flowrate, the greater the temperature increases. The injection duration is shorter at the higher flowrate, because the injection volume is limited to the capacity of the machine.

The power law can predict the temperature measurements as well as the Cross law, as the power law is drawn from the critical viscosity points identified using the temperature variations of the Cross-law simulations. Indeed, the heat generated by viscosity dissipation within the flow is brought to the central axis by convection. The viscosity of the flow affects not only the viscous dissipation power (shear rate multiplied by shear stress), but also the velocity field (integral of shear rate) for the convection.

The steady-state shear rate profiles (at $42.4 \text{ cm}^3 \cdot \text{s}^{-1}$ and $56.5 \text{ cm}^3 \cdot \text{s}^{-1}$) as a function of radial position in the annular structure, are calculated respectively with the Cross law and the power law and presented in Fig. 5. The radius of the central axis (inner radius of the annular flow) is 4 mm. The outer radius of the annular flow is 10 mm.

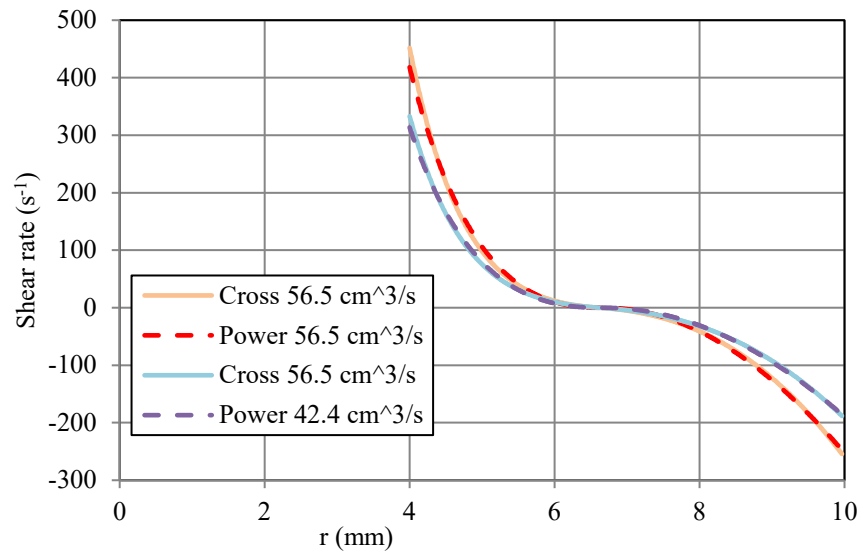


Fig. 5. Steady-state shear rate profiles as a function of radial position in the annular structure, calculated respectively with the Cross law and the power law, at $42.4 \text{ cm}^3 \cdot \text{s}^{-1}$ and $56.5 \text{ cm}^3 \cdot \text{s}^{-1}$.

The power-law calculations show lower absolute values of shear rate close to the inner and outer walls ($r = 4 \text{ mm}$ and 10 mm) of the annular geometry, compared to those of the Cross law. However, for example at $r = 5 \text{ mm}$ in the flow, the absolute values of shear rate obtained by the power law become higher than the Cross-law results. Although these differences are minuscule, they reveal that the power-law parameters that we identified with the innovative method minimize the prediction error across a certain depth of the flow domain.

The shear rates of the critical points in Fig. 3 are 61.7 s^{-1} and 80.5 s^{-1} . They have lower values than the maximum shear rates in the annular flow in Fig. 5. The maximum shear rates are on the surface of the central axis ($r = 4 \text{ mm}$):

- 333 s^{-1} at the flowrate of $42.4 \text{ cm}^3 \cdot \text{s}^{-1}$;
- 452 s^{-1} at the flowrate of $56.5 \text{ cm}^3 \cdot \text{s}^{-1}$.

The power law is capable of delivering accurate predictions, because the power-law curve in Fig. 3 remains close to the Cross-law curve at the shear rate of 452 s^{-1} . The viscous dissipation method does not identify a power-law curve to fit the high-shear region beyond the maximum shear rate in the flow. By not doing so, the identified power law has less error in the relatively low-shear region (from 20 to 60 s^{-1}) on the left side of the critical points in Fig. 3.

Since the viscosity depends on the shear rate for non-Newtonian materials such as the polymers, we can plot the viscosity profile as a function of radial position in Fig. 6a. The main criticism of using the power law is that when a zero shear rate exists in the flow (Fig. 5), the calculated viscosity will reach a high or even infinite value in the low-shear region (Fig. 6a), which is not physical. However, Fig. 6b shows that the calculated shear stress (obtained by multiplying the shear rate by the viscosity) is not affected by the « zero shear rate problem » of the power law.

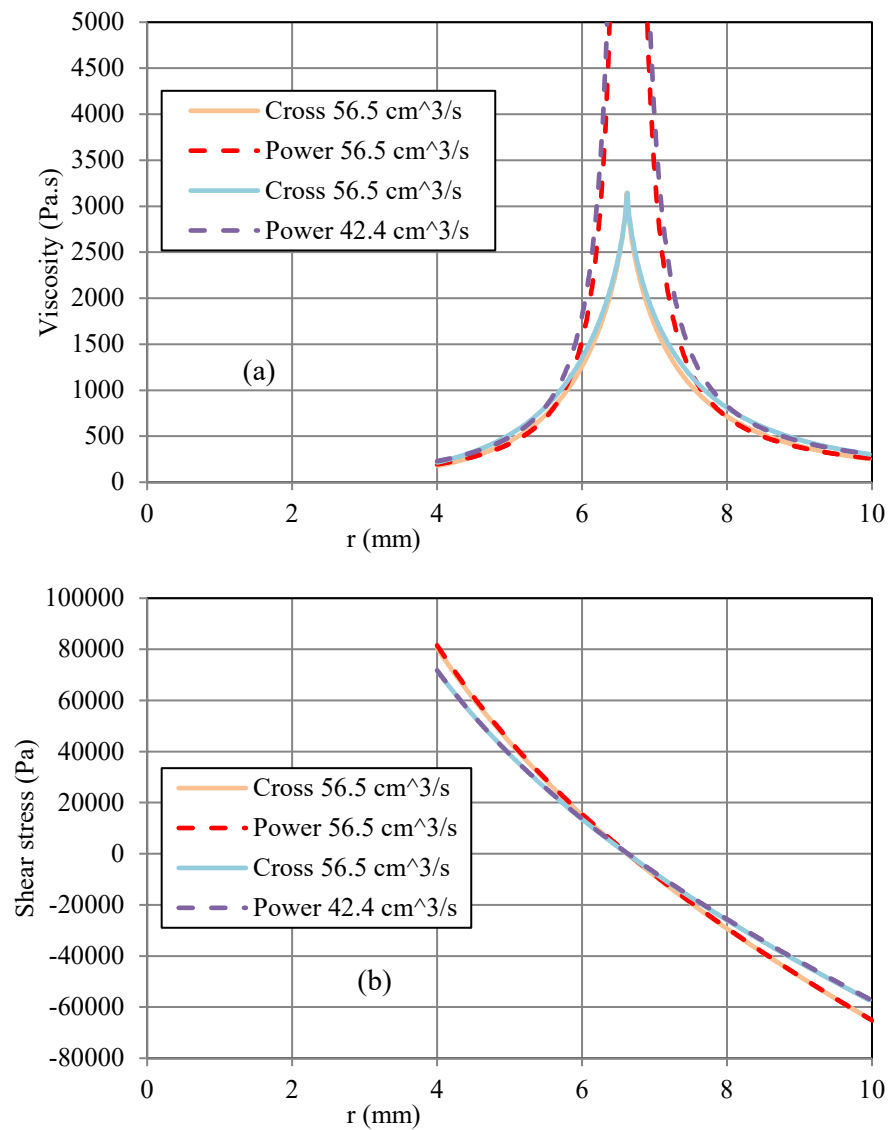


Fig. 6. Steady-state (a) viscosity and (b) shear stress profiles as a function of radial position in the annular structure, calculated respectively with the Cross law and the power law, at 42.4 cm³.s⁻¹ and 56.5 cm³.s⁻¹.

The velocity profiles are presented in Fig. 7. The predictions of the Cross law and the power law are almost the same on the velocity fields.

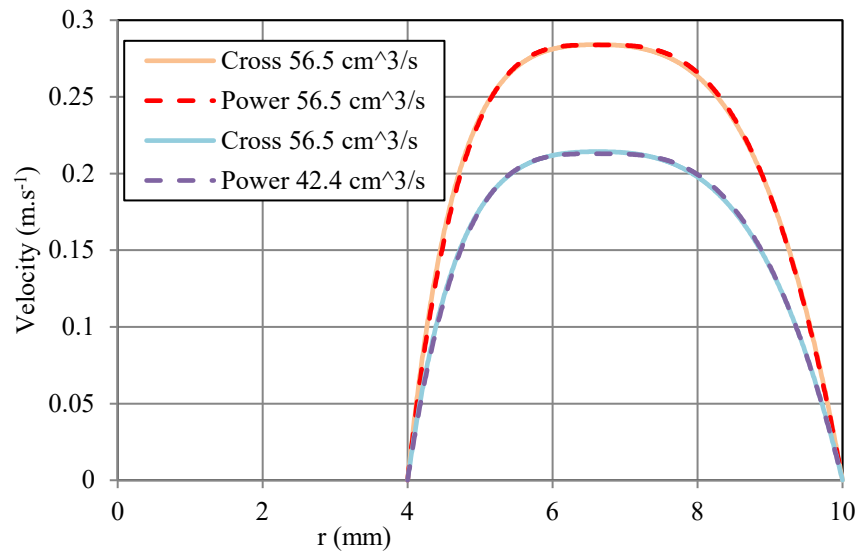


Fig. 7. Steady-state velocity profiles as a function of radial position in the annular structure, calculated respectively with the Cross law and the power law, at $42.4 \text{ cm}^3 \cdot \text{s}^{-1}$ and $56.5 \text{ cm}^3 \cdot \text{s}^{-1}$.

Fig. 7 shows again that the power-law parameters identified using the viscous dissipation method minimize the prediction error across a certain depth of the flow domain. This new method aims to identify parameters to reproduce the same heat exchange between the flow and the central axis of the annular geometry, rather than focusing on the pressure loss (like the classic capillary rheometry method [10]). Viscous dissipation and velocity profile are two of the key factors in this heat exchange.

If we aim to identify the power-law parameters using the simulated pressure measurements corresponding to each flowrate ($42.4 \text{ cm}^3 \cdot \text{s}^{-1}$ and $56.5 \text{ cm}^3 \cdot \text{s}^{-1}$) to solve the pressure-flowrate equation of annular flow [11], this power law, different from the one identified with the viscous dissipation method, will be more accurate for pressure loss predictions but can be less accurate to predict velocity profiles especially at the center of the flow (« Power* » in Fig. 8). In general, the power-law calculations in Fig. 8 are still close to the Cross-law calculations. The power law identified with pressure measurements can have good performance as well.

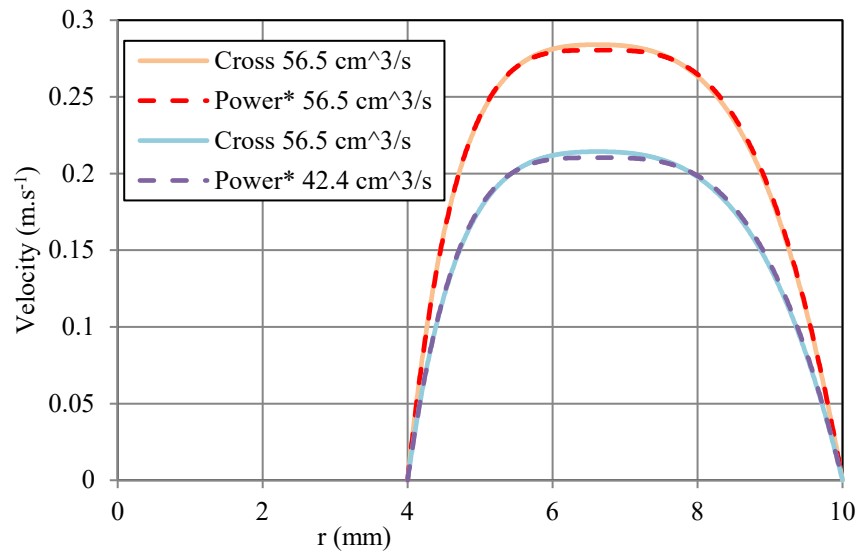


Fig. 8. Steady-state velocity profiles as a function of radial position in the annular structure, calculated respectively with the Cross law and the power law (identified with the pressure method), at $42.4 \text{ cm}^3 \cdot \text{s}^{-1}$ and $56.5 \text{ cm}^3 \cdot \text{s}^{-1}$.

The velocity values can be divided by the average velocity to obtain a dimensionless velocity profile. For a power-law type material, the dimensionless velocity profile depends on the value of the index $n_p = [\partial \ln \eta / \partial \ln \dot{\gamma}]$, and does not depend on the flowrate [8,11]. For a Cross-law type material, the dimensionless velocity profile depends on the flowrate. In Fig. 9, a power-law type dimensionless velocity profile is drawn to compare with Cross-law ones for a large range of flowrates.

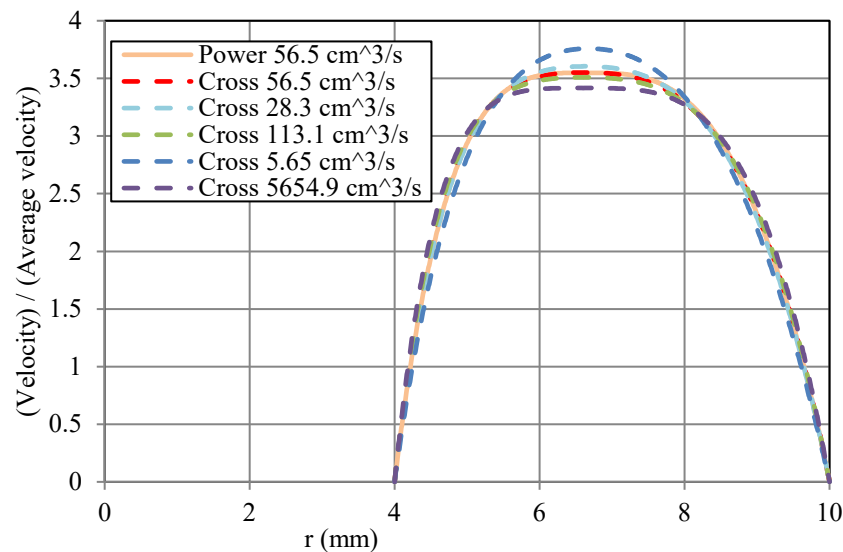


Fig. 9. Dimensionless steady-state velocity profiles as a function of radial position in the annular structure, calculated respectively with the power law (identified with the viscous dissipation method) and the Cross law for a large range of flowrates.

The power law identified with the viscous dissipation method is used to obtain the power-law type dimensionless velocity profile in Fig. 9. When the flowrate at $56.5 \text{ cm}^3 \cdot \text{s}^{-1}$ is multiplied or divided by two. The Cross-law type profiles are still close to the power-law one. When the flowrate is 100 times higher or 10 times lower, differences become significant.

Fig. 9 indicates that the identified local power law has a certain range of validity. For a different range of flowrates, the local power law may need to be re-identified. For example, a local power law with n_p close to 1 will give better results at low flowrates when the material is almost Newtonian. When the local power law is identified at high shear rate regime, it will have a larger range of validity compared to the one identified in the Newtonian-shear thinning transition region (Fig. 3). In this study, the flowrates ($42.4 \text{ cm}^3.\text{s}^{-1}$ and $56.5 \text{ cm}^3.\text{s}^{-1}$) are chosen on purpose to obtain critical viscosity points in the Newtonian-shear thinning transition region, to show the potential of a power law which fits the Cross law only in a specific range.

Summary

An innovative viscous dissipation method is used to define an equivalent power-law curve from a Cross-law one. The temperature variations due to viscous dissipation, calculated by the power law and the Cross law, are both found to be accurate compared to the experimental measurements. Thanks to numerical tools, the shear rate, viscosity, shear stress and velocity profiles in the flow, respectively obtained with the Cross model and the power-law model, are compared. The comparisons show that it is possible to find a power law to approach to a Cross-law flow for a specific flowrate range. On the viscosity curve, this refers to a dominant functional segment for a specific shear rate range.

Although the calculated power-law flow can be close to the Cross-law one, the power law cannot reproduce exactly the same result of the Cross law. Using different methods to identify the power-law parameters lead to different calculation precisions in the flow domain.

In general, the power law can have competitive performance compared to the Cross law, when the power-law parameters are carefully chosen for a functional shear rate range of the material, even for the transition region between the low-shear Newtonian zone and the high-shear pseudo-plastic zone. This conclusion can be extended to other viscosity models, as long as they can be decomposed into straight line segments in logarithmic scale.

Acknowledgement

This work was supported by the French Ministry of Higher Education, Research and Innovation and held in IUT Nantes.

This work used Polypropylene PPC 9642 kindly supplied by the company TotalEnergies.

References

- [1] W. Ostwald, About the rate function of the viscosity of dispersed systems, *Kolloid Z.* 36 (1925) 99-117.
- [2] A. de Waele, Viscometry and plastometry, *Journal of Oil and Colour Chemists' Association.* 6 (1923) 33-88.
- [3] A.G. Fredrickson, Flow of non-Newtonian fluids in annuli, PhD Thesis, University of Wisconsin-Madison, 1959.
- [4] R.B. Bird, Experimental tests of generalised newtonian models containing a zero-shear viscosity and a characteristic time, *The Canadian J. Chem. Eng.* 43 (1965) 161-168. <https://doi.org/10.1002/cjce.5450430402>
- [5] D.W. McEachern, Axial laminar flow of a non-Newtonian fluid in an annulus, *AIChE J.* 12 (1966) 328-332.
- [6] M.M. Cross, Rheology of non-Newtonian fluids: a new flow equation for pseudoplastic systems, *J. Colloid Sci.* 20 (1965) 417-437.
- [7] P.J. Carreau, Rheological equations from molecular network theories, *Trans. Soc. Rheol.* 16 (1972) 99-127.

- [8] Q. Lin, N. Allanic, R. Deterre, P. Mousseau, M. Girault, In-line viscosity identification via thermal-rheological measurements in an annular duct for polymer processing, *Int. J. Heat Mass Transf.* 182 (2022) 121988. <https://doi.org/10.1016/j.ijheatmasstransfer.2021.121988>
- [9] Q. Lin, N. Allanic, P. Mousseau, Y. Madec, G. Beau, R. Deterre, On-line melt temperature measurements for polymer injection molding through an instrumented annular duct, *Polym. Eng. Sci.* 62 (2022) 3994-4004. <https://doi.org/10.1002/pen.26161>
- [10] B. Rabinowitsch, Über die viskosität und elastizität von solen, *Zeitschrift Für Physikalische Chemie.* 145 (1929) 1-26.
- [11] R. Deterre, F. Nicoleau, Q. Lin, N. Allanic, P. Mousseau, The flow of power-law fluids in concentric annuli: A full analytical approximate solution, *J. Non-Newtonian Fluid Mech.* 285 (2020) 104392. <https://doi.org/10.1016/j.jnnfm.2020.104392>